ISSN 0554-6397
Stručni članak
(*Professional paper*)

Ivan Ćatipović
E-mail: ivan.catipovic@fsb.unizg.hr
Tomislav Prosinečki
E-mail: tomislav.prosinecki@fsb.unizg.hr
Antonio Mikulić
E-mail: antonio.mikulic@fsb.unizg.hr
Smiljko Rudan
E-mail: smiljko.rudan@fsb.unizg.hr
University of Zagreb, Faculty of Mechanical Engineering and Naval Architecture, Ivana Lučića 5, Zagreb, Croatia

Wave Loads and Motions of Floating Bodies in Close Proximity

Abstract

The engineering problem of floating bodies positioned in close proximity and exposed to sea waves arises in cases of novel structures, such as floating photovoltaics, and traditional offshore structures, like a floating natural liquefied gas terminal, during the transfer of gas from a gas carrier to a gas storage and regasification unit. An integral part of the design of such structures is calculating loads and motions due to the incident waves. The calculation includes the assessment of first-order wave forces as well as hydrodynamic reactions, i.e. the added mass and the radiational damping. The calculation is based on potential flow theory, utilising the three-dimensional boundary element method. Compared to the case of one floating body, the case of multiple bodies is more complex because it contains 6N degrees of freedom, where N represents the number of observed floating bodies. Therefore, the hydrodynamic coefficients and the incident wave forces must account for the interaction between the floating bodies. The paper presents the calculations done for floating pontoons (intended for carrying the photovoltaic panels) and for a floating storage regasification unit (FSRU) with a liquefied natural gas (LNG) carrier.

Keywords: wave-induced motions, floating bodies in close proximity, boundary element method, potential flow

1. Introduction

Estimating wave loads and motions of offshore structures and vessels is crucial for operational safety in rough seas. This is based on the motion equation of a floating body derived from Newton's second law, where external loads are balanced with inertial forces [1]. Sea state is modelled as a random process resolved by spectral analysis. Typically, seakeeping estimates focus on a single floating body. Conversely, this paper aims to present estimates of motion and loads for closely spaced floating bodies that interact hydrodynamically.

This paper is partly motivated by floating Liquefied Natural Gas (LNG) terminals where a Floating Storage and Regasification Unit (FSRU) is used. It specifically considers the scenario where liquefied gas is transferred from an LNG carrier to an FSRU, as detailed in [2]. This typically occurs in a side-by-side setup, where the LNG carrier and FSRU are positioned close together, as noted in [3]. Such proximity of the vessels results in hydrodynamic coupling, which must be considered when estimating wave loads and motions [4].

The motivation also originates from floating photovoltaic (FPV) installations, which consist of multiple connected floating bodies. Incoming waves will cause structural loads on the floats and the connections between them [5]. Thus, the connections between floats are part of the numerical models, enabling realistic coupled responses. In [6], ball connections are modelled in a frequency-domain seakeeping model with an additional stiffness matrix to reflect their influence on multi-float motions and wave loads. In [7], the support structure was discretised into multiple floating bodies linked by elastic beams. In [8], it is proposed to use rubber rings and pads as connections for two triangular floats, where loads are determined via time-domain simulations. In [9], non-linear effects like viscous and drag forces were included, considering flexible connections from tests, to support the world's largest 5 MW floating PV farm in Singapore. Such models addressed hydrodynamic interactions, which are computationally intensive. So, [10] suggested a cut-off scheme to simplify calculations by neglecting interactions between bodies beyond a certain distance.

According to the current literature, the calculation of wave loads and motions is based on potential flow theory, utilising the three-dimensional boundary element method. Compared to the case of a single floating body, the case of multiple bodies is more complex because it involves $6N$ degrees of freedom, where N represents the number of observed floating bodies [6]. In this approach, when evaluating wave loads, there are first-order and second-order wave forces. First-order forces share the same frequencies as the incident waves. In contrast, second-order forces occur at much lower frequencies, which can be calculated as the differences between the frequencies of the incident waves. Additionally, second-order forces include a constant component known as drift forces [11].

As a part of estimating the motions, the hydrodynamic reaction, i.e. added mass and radiational damping, needs to be evaluated. In combination with the first-order

forces, the motion of the floating bodies can be assessed through the analyses in the frequency domain [1,11]. These types of motions, also called first-order motions, are relevant for offshore structures and vessels when estimating their operability. In combination with the first-order forces, they are used for assessing the structural integrity of observed floating bodies. On the other hand, the second-order forces, which are also determined by the numerical methods based on the potential theory [11], are relevant when considering the mooring system that is necessary for station keeping of floating bodies [12,13]. Such analyses are done by time domain simulations.

The study presented here is the continuation of the work presented in [6] and [14], where the theoretical background of the appropriate methodology is described along with a comparison with available experimental results. In more detail, the development of the connection stiffens matrix for ball joints between floating bodies is presented in [6]. The comparison of the numerical and experimental results of the wave induced motions and loads for two rectangular barges is given in [14]. In this paper, the focus is on the calculations, or more precisely, the calculation results of wave loads and motions of the first order for floating bodies in close proximity. Firstly, the results for an FSRU with an LNG carrier during liquefied gas reloading are shown. Secondly, the results for connected floating bodies, which serve as carriers of photovoltaic (PV) systems, are provided. The case studies are given in Chapter 3, while Chapter 2 brings only a brief presentation of the applied methodology.

2. Mathematical model

A body oscillating on a wave is in the dynamic equilibrium defined by Newton's second law. The equation of motion of a floating rigid body with 6 degrees of freedom (DOF) of motion is defined by this law. With the assumption of the harmonic wave forcing, the motion equation can be derived to be convenient for the frequency domain analysis as follows, [1,11].

$$\left(-\omega^2\left(\left[M\right]+\left[A\right]\right)+i\omega\left[B\right]+\left[K\right]+\left[C\right]\right)\left\{\delta\right\}=\left\{F\right\} \tag{1}$$

where $[M]$ is the mass matrix due to its own body mass, while $[A]$ is the added mass matrix. The added mass models the inertial forces from seawater as the body accelerates. $[B]$ represents radiational damping from outgoing waves. Hydrostatic stiffness from buoyancy and weight is denoted by $[K]$. First-order wave forces are given by $\{F\}$ while the vector $\{d\}$ gives, after solving the equation, the 6DOF motions of a floating body.

The matrix $[C]$ is additional to the usual form of the equation. It can be used to introduce the linearised forces of the mooring system acting on a body and has a size of 6×6, the same as other matrices in the equation. In a case where multiple floating bodies are observed, a special form of the matrix $[C]$ can be used to model the mechanical connections between the bodies [6]. In such a case, the matrix $[C]$ has a size of $6N$×$6N$

where N is the number of bodies. Likewise, all other matrices in the motion equation that have such size, i.e., the matrices [M], [A], [B], and [K], have a size of $6N\times\boldsymbol{6N}$, and the wave force vector {F} is 6N×1 if multiple bodies are observed.

Determination of [A], [B] and {F} is based on potential flow theory. This flow is non-viscous, irrotational, incompressible and homogeneous, and it is assumed that there are no cavitation gas bubbles in the fluid [15]. In a case of floating bodies in close proximity, the added mass matrix[A] introduces the hydrodynamic coupling regarding the inertial forces due to seawater, meaning that the acceleration of one body will exert the inertial forces on all bodies in the system, including itself. Similarly, the damping matrix [B] will introduce the damping forces on all bodies if one body moves with a specific velocity. Furthermore, when the wave forces, given in {F}, are determined for one of the bodies, the presence of all other bodies is considered, [15]. Finally, solving such a motion equation will provide the motion of all bodies, i.e., the vector {d} comprises the 6 DOF motions of all the bodies (so has a size of $6N\times\boldsymbol{1)}$ with inclusion of the hydrodynamic coupling between the floating bodies.

The presented mathematical model neglects the fluid's viscosity. The main drawback of this methodology is observed in the calculated roll motions of a ship. This results in significant overestimates of the roll motions. To mitigate this drawback, the viscous damping is modelled as a certain percentage of the critical damping and added to the matrix [B], [11,15]. Another issue that originates from neglecting the fluid's viscosity is the so-called gap resonant wave elevation, which occurs when a multiple floating body system is observed [16]. The resonant elevation is noticed in the calculations in the gaps between the floating bodies. As a direct consequence of neglecting the fluid's viscosity, the wave elevation in the gaps is significantly overestimated, which leads to the overestimation of the wave forces. A practical approach to resolve the issue is to introduce additional panels in the gaps at the still water surface level [3,4]. The panels are of a special type and are developed to dampen the wave elevation, where a coefficient defines the level of the damping. If the coefficient is set to 0, there is no damping at all, while the full damping is achieved when the coefficient is set to 1.

3. Case studies

3.1. FSRU and LNG carrier

As already noted, during the transfer of liquefied gas from an LNG carrier to an FSRU, these vessels are in a side-by-side configuration, i.e. in close proximity, so an analysis of the wave motions and loads should incorporate the hydrodynamic coupling. The results of such analyses are an essential part of the design of a mooring system, or more specifically, when the tensions in mooring lines are calculated. It is important to note that the second-order wave forces, not considered in this study, are also key factors in the analysis of the mooring system.

In this case study, to determine the wave motions and loads on the FSRU and LNG carrier, the linear seakeeping software package HydroStar [17], which combines the potential flow theory and boundary element method, is used. Firstly, the calculations are done on a single FSRU. The mesh model of the FSRU is given in Figure 1, while Figure 2 shows the FSRU and LNG carrier in a side-by-side configuration. For each vessel, approximately 4000 boundary elements, i.e. panels, are used. Table 1 brings their main dimensions. In this case study, it is assumed that the FSRU and LNG carrier are of the same size. The distance between them is assumed to be 4.5 m. The FSRU is set at displacement draft in the calculations, whereas the LNG carrier is at a fully loaded draft. The depth of the site is 17.4 m. The azimuth of the vessels in consideration is 225°. The roll viscous damping is set at 4% of the critical damping, while the gap resonance damping is set to 0.03. The mooring system is not considered in the calculations.

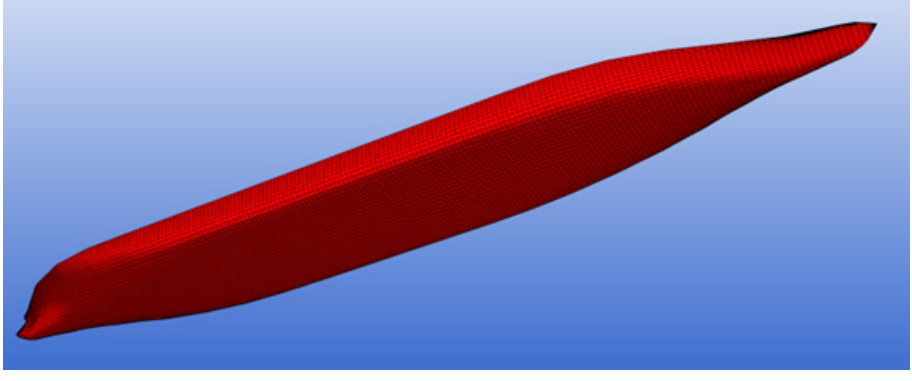

Figure 1. Mesh model of the single FSRU

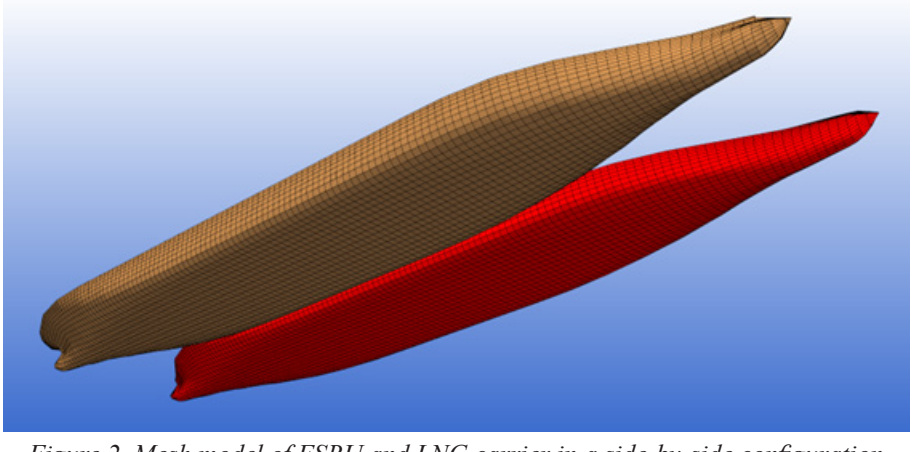

Figure 2. Mesh model of FSRU and LNG carrier in a side-by-side configuration

Figures 3, 4 and 5 gives the significant values of the heave, roll and pitch motions, respectively. The values are shown in relation to incoming wave directions given in degrees with respect to North, clockwise. On each figure, there are values for a single FSRU along with values for the FSRU and LNG carrier in side-by-side configuration. Similarly, Figures 6, 7 and 8 show the calculated results regarding surge and sway forces and yaw moment.

Table 1. The main dimensions of the FSRU and LNG carrier

Description	FSRU/LNG carrier	Unit
Length overall	283.0	m
Length between perpendiculars	264.0	m
Beam	42.0	m
Draft fully loaded	11.2	m
Draft in ballast	9.2	m

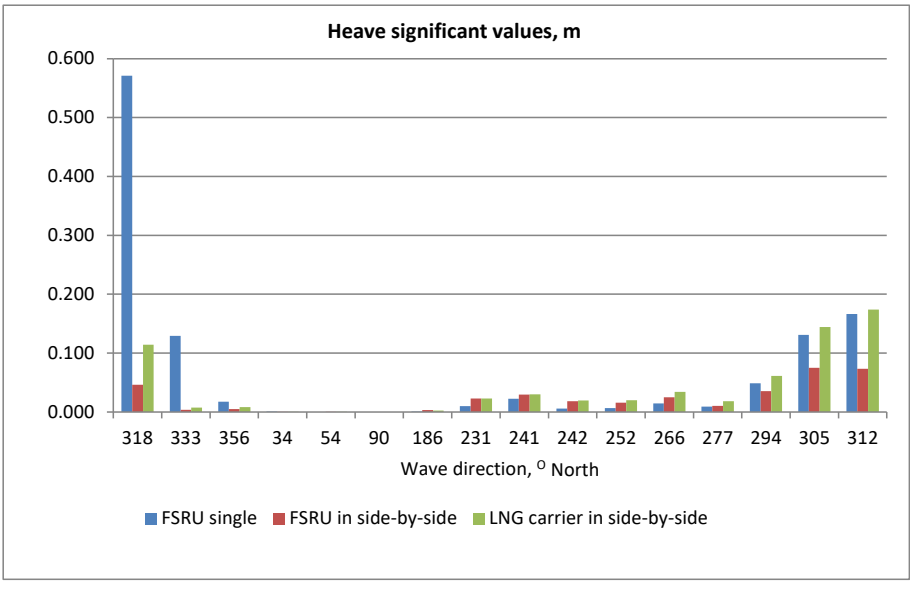

Figure 3. Heave significant values for a single FSRU and FSRU and LNG carrier in a side-by-side configuration

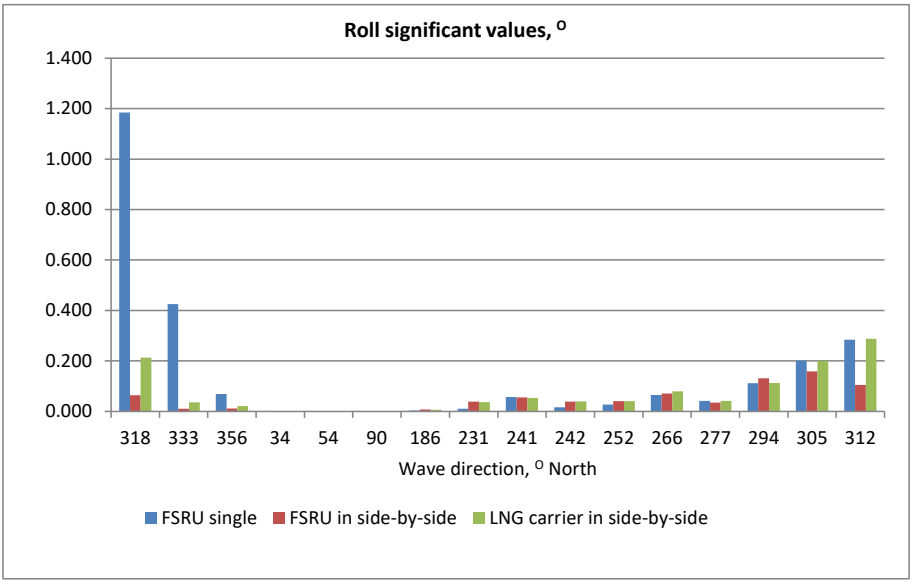

Figure 4. Roll significant values for a single FSRU and FSRU and LNG carrier in a side-by-side configuration

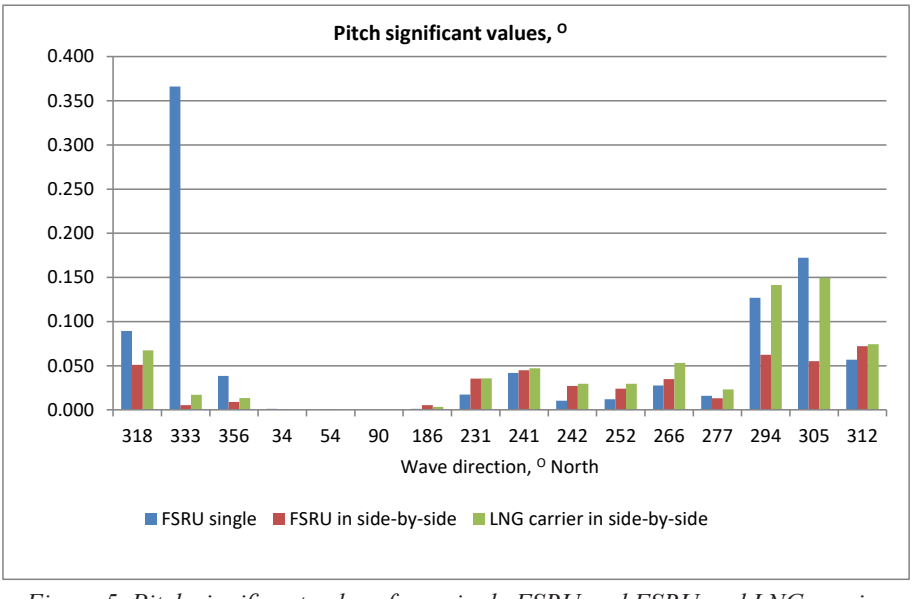

Figure 5. Pitch significant values for a single FSRU and FSRU and LNG carrier in a side-by-side configuration

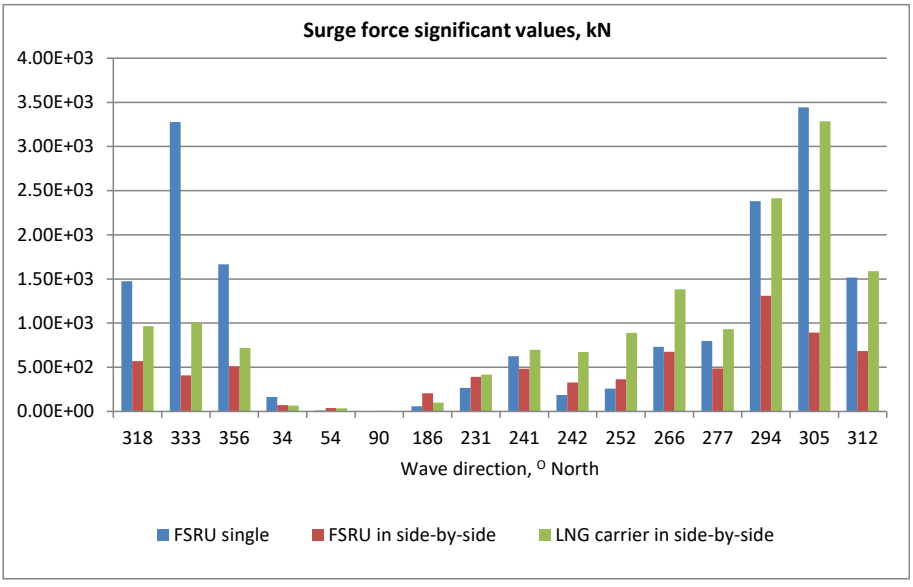

Figure 6. Surge force significant values for a single FSRU and FSRU and LNG carrier in a side-by-side configuration

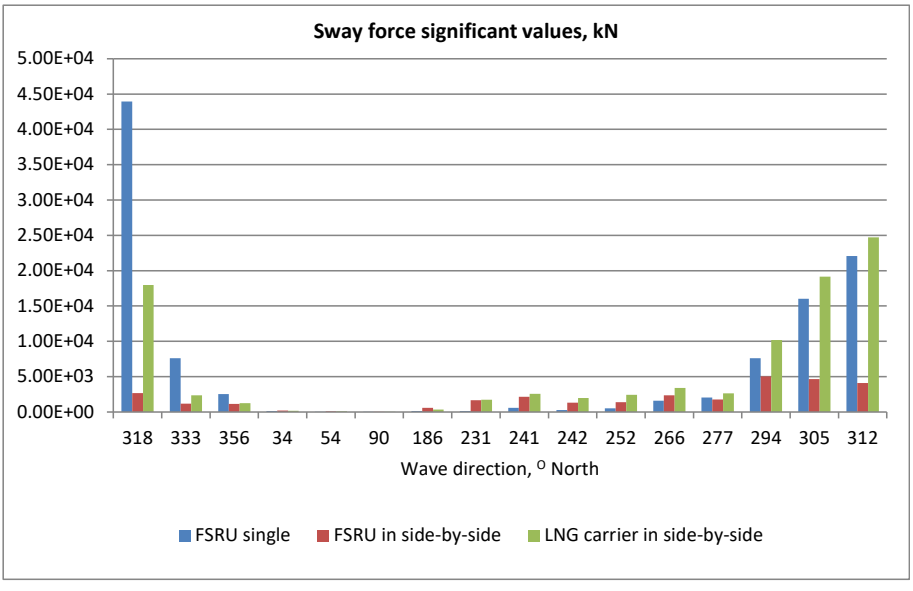

Figure 7. Sway force significant values for a single FSRU and FSRU and LNG carrier in a side-by-side configuration

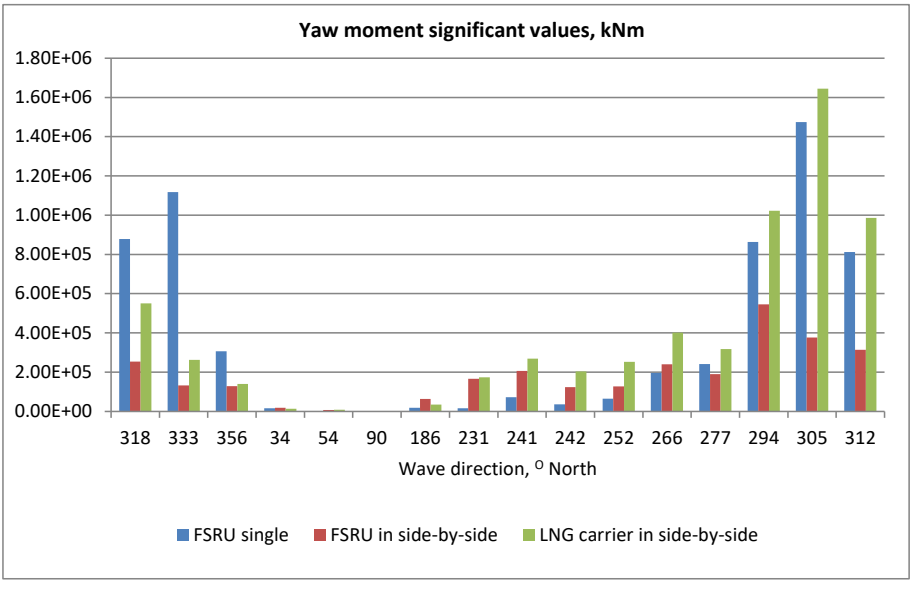

Figure 8. Yaw moment significant values for a single FSRU and FSRU and LNG carrier in a side-by-side configuration

This case study showed that the wave motion and loads significantly vary if the FSRU is observed solely or in a side-by-side configuration with the LNG carrier on irregular waves. Also, in many cases, or in many wave directions, the vessel that is exposed directly to waves experiences higher significant values of the motion and loads than the shielded vessel. However, in some cases, the vessel exposed directly to waves (in the side-by-side configuration) has higher significant values of the motions or loads than the same vessel if observed solely. In such circumstances, the shielded vessel acts as an amplifier of the motions and loads of the exposed vessel.

3.2. Connected floating bodies

This case study was done on a set of connected floating bodies, i.e. pontoons, which serve as carriers of PV panels [6]. The dimensions of the individual pontoon can be found in Figure 9. Figure 10 shows the arrangement and numbering of the pontoons, along with the coordinate system used in the calculations. In the calculations, it is assumed that the pontoons are connected by ball joints as presented in [6]. The bodies are spaced apart 700 mm. In total, nine bodies are observed. The mesh of the whole system is presented in Figure 11.

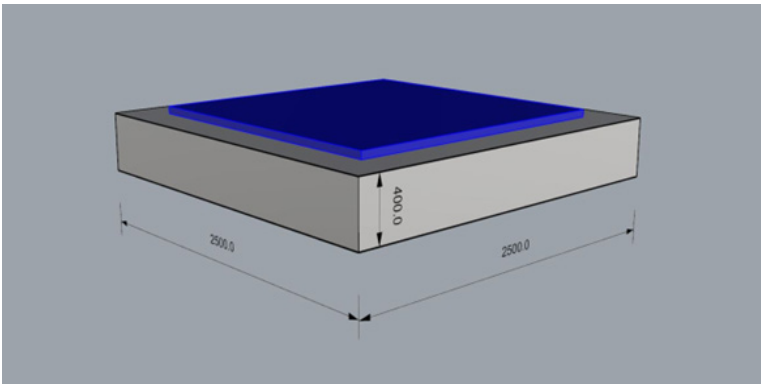

Figure 9. The main dimensions of the individual floating body

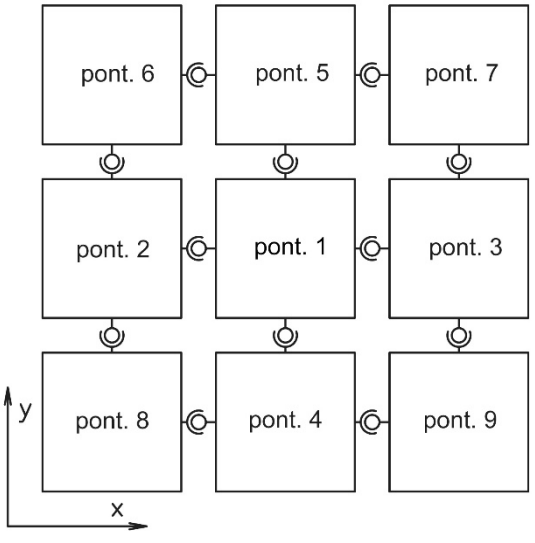

Figure 10. The arrangement and numbering of floating pontoons

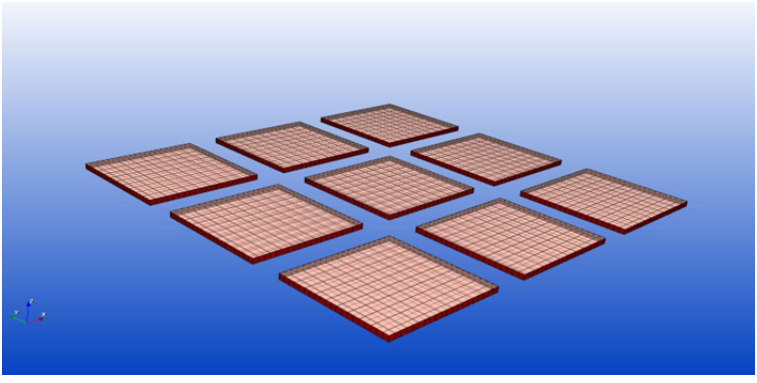

Figure 11. Mesh of the floating bodies.

The following figures show the response amplitude operator (RAO) for the pitch motions. Figures 12, 13 and 14 show the pitch RAO for the pontoons in the middle, i.e. the pontoons numbered 2,1 and 3. The RAO values are related to the incoming wave directions (in degrees), where 0° coincides with the x-axis of the global coordinate system (as presented in Figure 10), while 90° is in line with the *y*-axis.

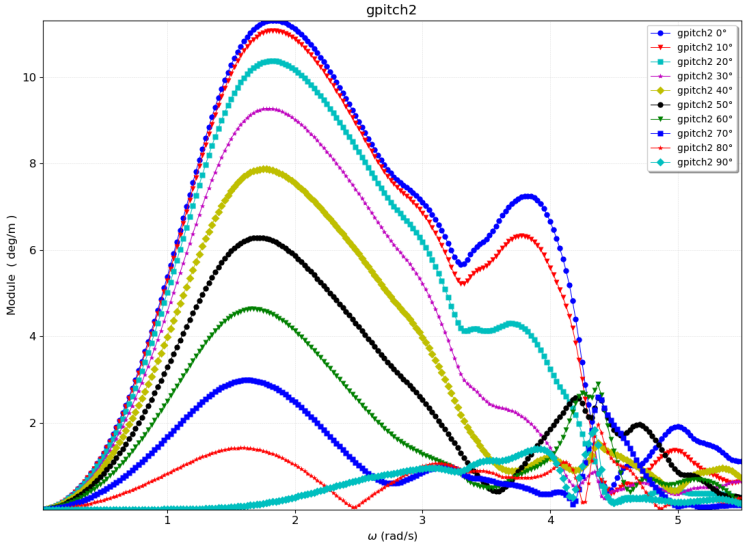

Figure 12. Pitch RAO for pontoon no. 2.

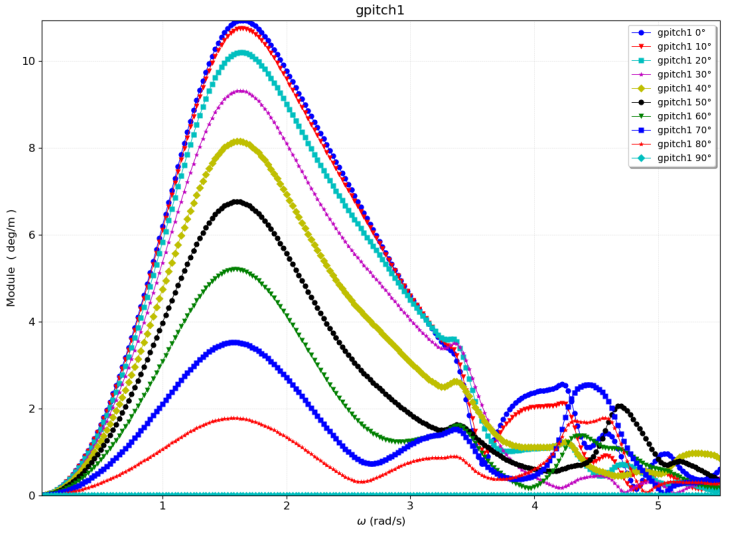

Figure 13. Pitch RAO for pontoon no. 1.

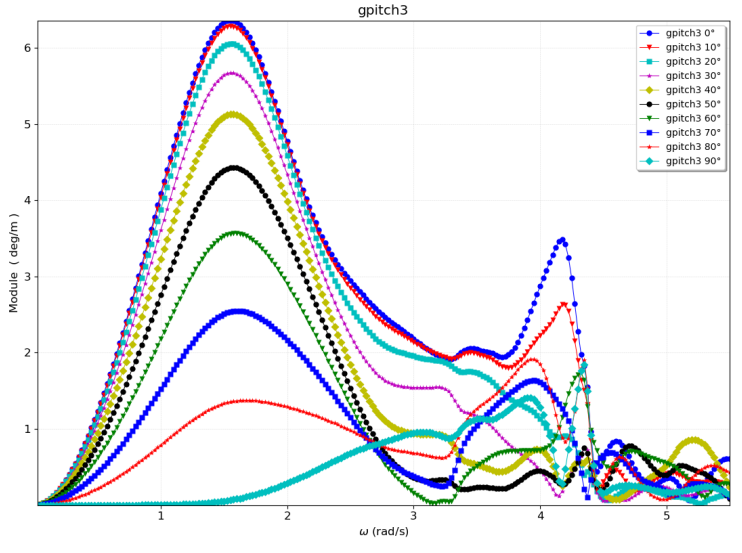

Figure 14. Pitch RAO for pontoon no. 3.

Figures 12, 13 and 14 reveal a strong dependency of the motions to the incoming wave frequency. If observed closely, the presented pitch RAOs, it can be found that for waves with lower frequencies (i.e. longer waves), the results are similar for the pontoon directly exposed to waves to the pontoon just behind and thus shielded. For higher frequencies, the difference is quite noticeable, i.e. the RAO values are significantly higher. Also, the significant shielding effect at lower frequencies is only noticeable for the third row of the pontoon following the incoming wave direction. Hence, the RAO values in the third-row pontoon are smaller than those in the pontoon located at the first and second rows. In the case of the higher frequencies, a non-intuitive occurrence is noticed, i.e. in general, the third-row pontoon has a higher pitch RAO velocity than the second-row pontoon.

4. Conclusions

In this paper, the calculation results of wave loads and motions of floating bodies in close proximity are presented in a case where a traditional offshore structure is observed, i.e. the FSRU and LNG carrier in a side-by-side configuration. A case of innovative floating structure made as a 3×3 array of connected floating bodies is also studied. For this purpose, the already developed methodology is applied, which incorporates the hydrodynamic coupling between the vessels. According to current literature, the methodology can deal with a specific challenge in the multiple body hydrodynamics calculations, the resonant wave elevation in the gaps between the bodies. The case studies revealed that there are significant differences in the wave motions and loads if the floating body is observed solely or in pair with another body in close proximity, which is not surprising. Also, it is not surprising that the shielding effects are found that causes lower values of the wave motions and loads of the body which is not directly exposed to the waves. This shielding effect is strongly dependent of the incoming wave frequency. However, in some specific wave conditions, the exposed body has larger motions and loads in comparison to case when observed solely. Here, it should be kept in mind that such results can originate from shortcomings of the used methodology and possibly are not the representation of real-world situations.

Acknowledgements

This work was supported by the Croatian Science Foundation under the project number HRZZ-IP-2022-10-4408.

References

1. Čorić, V., Prpić-Oršić J.: Pomorstvenost plovnih objekata; Zigo, Rijeka, 2006.
2. Ye, W., Luo, Y., Pollack, J.: LNG Floating Regasification Unit (FRU) Side-by-Side Mooring Analysis, 24th International Conference on Offshore Mechanics and Arctic Engineering (OMAE 2005), Halkidiki, Greece, 2005.
3. Huijsmans, R.: Advances in the Hydrodynamics of Side-by-Side Moored Vessels, Proceedings of the 26th International Conference on Offshore Mechanics and Arctic Engineering (OMAE 2007), San Diego, California, USA, 2007.
4. Bunnik, T., Pauw, W., Voogt, A.: Hydrodynamic Analysis for Side-by-Side Offloading, Proceedings of the 19th International Offshore and Polar Engineering Conference (ISOPE 2009), Osaka, Japan, 2009.
5. Ćatipović, I., Alujević, N., Smoljan, D., Mikulić, A.: A Review on Marine Applications of Solar Photovoltaic Systems, Proceedings of the 15th International Symposium on Practical Design of Ships and Other Floating Structures (PRADS 2022), Dubrovnik, Croatia, 2022.
6. Ćatipović, I, Ilić, L., Mikulić, A., Smoljan, D.: Seakeeping assessment of a floating object with installed photovoltaic system, Sustainable Development and Innovations in Marine Technologies – Proceedings of the 19th International Congress of the International Maritime Association of the Mediterranean (IMAM 2022), Istanbul, Turska, 2022.
7. Shi, Y., Wei, Y., Tay, Z. Y., Chen, Z.: Hydroelastic analysis of offshore floating photovoltaic based on frequency-domain model. Ocean Engineering, Volume 289, Part 1, 2023, 116213.
8. Kang, W., Lian, Z. and Han, Y.: Design and Hydrodynamic Performance Analysis of a Two-module Wave-resistant Floating Photovoltaic Device, Journal of Physics: Conference Series - 7th International Conference on Hydrodynamics, Energy and Electric Power System, Beijing, China, 2023.
9. Zhang, C., Dai, J., Ang, K. K., Lim, H. V.: Development of compliant modular floating photovoltaic farm for coastal conditions, Renewable and Sustainable Energy Reviews, Volume 190, Part A, 2024, 114084.
10. Zhang, D, Du, J, Yuan, Z, Zhang, M, Zhu, F.: Hydrodynamic Modelling of Modularized Floating Photovoltaics Arrays, Proceedings of the ASME 2023 42nd International Conference on Ocean, Offshore and Arctic Engineering. Volume 8: Ocean Renewable Energy, Melbourne, Australia, 2023.
11. Faltinsen, O.M., Michelsen, F.C.: Motions of Large Structures in Waves at Zero Froude Number, International Symposium: The Dynamics of Marine Vehicles and Structures in Waves, 1974.
12. API RP 2SK: Design and Analysis of Stationkeeping Systems for Floating Structures, American Petroleum Institute, 3rd Edition, Washington, October 2005.
13. Bureau Veritas, Marine & Offshore Division: NR493 R03: Classification of Mooring Systems for Permanent and Mobile Offshore Units, Paris, 2015.
14. Ćatipović, I., Martić, K., Alujević, N. Rudan, S.: Hydrodynamic Forces and Reactions of Two Floating Bodies in Close Proximity. Pomorski zbornik, 62 (1), 2022, 57-74.
15. Faltinsen, O.M.: Sea Loads on Ships and Offshore Structures, Cambridge University Press, 1993.
16. Molin, B., Remy, F., Camhi, A., Ledoux, A.: Experimental and numerical study of the gap resonances in-between two rectangular barges, Congress of Intl. Maritime Assoc. Of Mediterranean IMAM 2009, Istanbul, Turkey, 12-15 Oct., 2009.
17. Bureau Veritas. HydroStar for Experts—User Manual; Bureau Veritas: Paris, France, 2018.